Analytical Methods

ROYAL SOCIETY OF CHEMISTRY

PAPER

View Article Online
View Journal | View Issue

Check for updates

Cite this: *Anal. Methods*, 2024, **16**, 4322

Experimental and numerical investigation of microdialysis probes for ethanol metabolism studies†

Tse-Ang Lee, [a] Jessie Peng,[a] Divjot Walia,[a] Rueben Gonzales[b] and Tanya Hutter *[ac]

Received 16th April 2024
Accepted 11th June 2024

DOI: 10.1039/d4ay00699b

rsc.li/methods

Microdialysis is an important technique for *in vivo* sampling of tissue's biochemical composition. Understanding the factors that affect the performance of the microdialysis probes and developing methods for sample analysis are crucial for obtaining reliable results. In this work, we used experimental and numerical procedures to study the performance of microdialysis probes having different configurations, membrane materials and dimensions. For alcohol research, it is important to understand the dynamics of ethanol metabolism, particularly in the brain and in other organs, and to simultaneously measure the concentrations of ethanol and its metabolites – acetaldehyde and acetate. Our work provides a comprehensive characterization of three microdialysis probes, in terms of recovery rates and backpressure, allowing for interpretation and optimization of experimental procedures. *In vivo* experiments were performed to measure the time course concentration of ethanol, acetaldehyde, and acetate in the rat brain dialysate. Additionally, the combination of *in vitro* experimental results with numerical simulations enabled us to calculate diffusion coefficients of molecules in the microdialysis membranes and study the extent of the depletion effect caused by continuous microdialysis sampling, thus providing additional insights for probe selection and data interpretation.

1. Introduction

Microdialysis, a widely used *in vivo* sampling technique suitable for conscious animals, offers a means of continuous analyte sampling through a catheter called a microdialysis probe. The probes are commonly designed in two configurations, concentric[1] and side-by side.[2] The probe features a semipermeable membrane at its tip, allowing passive diffusion of analytes from the target tissue. The probe is continuously perfused with a solution (perfusate) that closely mimics the ionic and chemical composition of the tissue fluid surrounding the probe. The resulting dialysate, the solution leaving the probe, is collected at specific time intervals for subsequent off-line analysis, which can include Fourier-transform infrared spectroscopy (FTIR),[3] gas chromatography with flame ionization detection (GC-FID),[4] liquid chromatography-mass spectrometry (LC-MS)[5] or capillary electrophoresis.[6] Microdialysis has proven successful for sampling a variety of analytes, including but not limited to adenosine,[7] glutamate,[8] inosine,[9] lactate,[10] and more.[11–13] This technique is particularly well-suited for the sampling of small extracellular water-soluble molecules such as ethanol and its primary metabolites. While the microdialysis technique is currently mainly used for research purposes, its use for clinical monitoring is important. For example, it is used for monitoring brain chemistry changes over time of hospitalized traumatic brain injury patients.[14,15]

For alcohol researchers, it is crucial to have a reliable method to sample ethanol and its metabolites *in vivo*, as both ethanol and its metabolites can lead to harmful effects.[16] Ethanol can be metabolized through various pathways, with the primary route involving alcohol dehydrogenase (ADH)-catalyzed oxidation to acetaldehyde.[17] Acetaldehyde itself is known to be genotoxic and carcinogenic, which likely contributes to the development of certain types of cancer.[18] Previous studies suggest that an elevated acetaldehyde concentration in the rat brain significantly induces behavioral effects that are characteristic of addictive drugs.[19] Furthermore, ADH-catalyzed oxidation forms one molecule of NADH, increasing respiratory chain activity, and thereby, oxygen use and reactive oxygen species formation.[20] The oxidation of ethanol to acetaldehyde can also be driven by cytochrome P4502E1 (CYP2E1) when large amounts of alcohol are consumed.[21] CYP2E1 metabolism causes a significant release of free radicals, weakening defenses

[a]*Department of Mechanical Engineering, The University of Texas at Austin, Austin, TX 78712, USA. E-mail: tanya.hutter@utexas.edu*

[b]*College of Pharmacy, Division of Pharmacology and Toxicology, The University of Texas at Austin, Austin, TX 78712, USA*

[c]*Materials Science and Engineering Program and Texas Materials Institute, The University of Texas at Austin, Austin, TX 78712, USA*

† Electronic supplementary information (ESI) available. See DOI: https://doi.org/10.1039/d4ay00699b

against oxidative stress. Acetaldehyde is metabolized into acetate by aldehyde dehydrogenase. Although acetate has a lower acute toxicity than acetaldehyde, acetate may also mediate some of ethanol's behavioral effects; the molecule easily crosses the blood–brain barrier and produces sedation and ataxia.[22] Furthermore, acetate might contribute to addictive behavior by regulating gene expression.[23] Therefore, quantification of ethanol and its metabolites is important for the investigation of concentration-dependent neuropharmacological changes in the brain that occur during ethanol consumption.

Previous work has shown that ethanol and its metabolites can be measured *in vivo* under various conditions. For example, microdialysis has been used in conjunction with gas chromatograph (GC) with flame ionization detection (FID) to measure ethanol concentrations in the nucleus accumbens of the rat's brain in three different rat lines *in vivo*.[24] GC-FID is highly sensitive to hydrocarbons and facilitates quantitative analysis of volatile organic compounds in headspace, often using the solid phase microextraction (SPME) technique.[25] Compared to gas chromatograph with mass spectrometry (GC-MS), GC-FID system is typically less expensive and easier to operate, which makes it suitable for routine analysis. Time course measurement of ethanol concentration has been performed during ethanol self-administration procedure using *in vivo* microdialysis.[4] Furthermore, microdialysis has also been used as a tool to quantify the concentration of ethanol to study the physiological and pharmacological effects of ethanol on the brain.[26–28] The technique has also been used to measure ethanol and acetaldehyde concentrations simultaneously in freely moving rats.[29] Acetate has been studied using microdialysis for determination of the pharmacokinetic properties of a chemotherapeutic agent.[30]

However, to date, ethanol, acetaldehyde, and acetate have not been simultaneously measured in the brain *in vivo*. Moreover, the extent of ethanol metabolism that may occur in the brain and contribute to acetaldehyde and acetate levels is still controversial. Acetate, a short chain fatty acid, is difficult to analyze using gas chromatograph because it is susceptible to tailing and may yield an irregular peak shape, and it has also been shown to produce ghosting on a gas chromatogram due to adsorption to the column.[31] Ghost peaks occur when analytes have lower-than-expected retention times, which is typically caused by confounding interactions with the mobile or stationary phase. Although methods to reduce ghosting of short chain fatty acids exist, such as adding formic acid to the mobile phase, or using a special porous polymer stationary phase, these modifications require specialized equipment and produce narrower linear ranges.[32] Microdialysis is capable of sampling the multiple compounds of interest in ethanol metabolism simultaneously. However, limitations of the analytical techniques may complicate simultaneous quantification. Other analytical techniques such as infrared spectroscopy (IR) have been used in conjunction with microdialysis for simultaneous measurement of glucose and lactate in traumatic brain injury patients.[3] Since ethanol, acetaldehyde, and acetate produce clear and distinct mid-IR spectra,[33] sampling with microdialysis and quantification with mid-infrared is a feasible approach.

In order to better understand and characterize the performance of microdialysis probes in different configurations, *in vitro* microdialysis experiments were performed. First, microdialysis experiments were performed with individual analytes – ethanol, acetaldehyde and acetate, to characterize three microdialysis probes having different membranes, configurations and dimensions. Then, to demonstrate the capability of quantifying the concentrations of the three molecules simultaneously, *in vitro* microdialysis measurements were performed on the mixture of the three compounds, and the collected sample was measured using infrared spectroscopy. To optimize the experimental design, the flow recovery rate was measured at different backpressures to determine the maximum pressure a probe can withstand without leading to erroneous results. *In vivo* microdialysis was performed to measure the time course ethanol and acetaldehyde concentration in rat brain after ethanol consumption based on the probe characteristics. Through computational modeling, the diffusion characteristics of ethanol, acetaldehyde and acetate in the dialysis membranes were numerically studied. The diffusion coefficient of the three compounds was estimated by fitting the experimental results to a three-dimensional (3D) model. The findings from this study will guide researchers to select appropriate probes for a particular application, thereby advancing the field of *in vivo* sampling and ethanol metabolism research.

2. Materials and methods

2.1. Materials and instruments

2.1.1. Microdialysis probes. Lab-made probes were fabricated using the same method described in a previous paper, which employed a side-by-side configuration.[34] In brief, two pieces of fused silica tubing were used for the inlet and outlet lines of the probe. Both pieces of tubing were inserted into a piece of regenerated cellulose membrane (Spectra/Por®) with a molecular weight cutoff (MWCO) of 13 kDa. The working distance of the probes was defined by the difference in length of the two pieces of silica tubing within the membrane. Epoxy was used to coat the portion of the membrane not used for dialysis, which determined the effective membrane length. For this study, probes with a 2 mm working distance were fabricated.

Additionally, two commercially available probes were used for direct comparison with the lab-made probe. One probe (MAB 4.15.2., Microbiotech/se AB, Stockholm, Sweden) had a 2 mm polyethersulfone (PES) membrane with a MWCO of 6 kDa. The other probe (CMA/11 14/01, Harvard Apparatus, Holliston, Massachusetts) had a 1 mm cuprophan membrane with the same MWCO of 6 kDa. Both of these probes have a concentric configuration.

2.1.2. Artificial cerebrospinal fluid (aCSF) and reagents. An artificial cerebrospinal fluid (aCSF) was prepared to simulate the chemical and ionic composition of the interstitial fluid of the brain, according to a previous study.[35] The concentration of each component was as follows: NaCl at 149 mM (Sigma, 1002755229), KCl at 2.8 mM (Fluka, 409316), $CaCl_2 \cdot 2H_2O$ at

1.2 mM (Sigma, 21097), $MgSO_4 \cdot 6H_2O$ at 1.2 mM (Sigma, 63068), ascorbic acid at 0.25 mM (Fluka, 95209), and glucose at 5.4 mM (Sigma, SLBV7620). Ethanol was obtained from Decon Labs (200 proof), while acetic acid (A6283) and acetaldehyde (402788) were both obtained from Sigma-Aldrich. All the solutions were prepared in aCSF.

2.1.3. Gas chromatography with flame ionized detector (GC-FID). A gas chromatograph (GC, Scion 436) equipped with a flame ionization detector (FID) and an 8400 Bruker autosampler was used to measure ethanol and acetaldehyde in the sample. The system consists of an HP Innowax capillary column (30 m × 0.53 mm × 1.0 μm film thickness), with hydrogen as the carrier gas with a flow rate set at 15 mL min^{-1}. A carboxen/PDMS coated solid phase micro-extraction (SPME) fiber (Supelco) was used for extraction and desorption, with times of 0.5 and 2 min for ethanol, and 5 and 5 min for acetaldehyde. The injection temperature was set to 280 °C. A circulating water bath was used to heat the sample carousel, and the sample vials were heated to 39.0 °C. The column oven temperature was set to 65 °C and 25 °C for ethanol and acetaldehyde, respectively. A sample volume of 2 μL was used. Calibration of the GC-FID using ethanol and acetaldehyde solutions at different concentrations is included in the ESI in Fig. S1,† where the measured detector signal is plotted as a function of concentration.

2.1.4. Ultraviolet-visible (UV-Vis) spectroscopy. Measuring acetate using gas chromatograph is challenging due to the need for a special column. Alternatively, ultraviolet-visible spectrophotometry has the ability to detect acetate at low mM levels. High sensitivity is important for the quantification of samples collected at high flow rates, which result in low recovery rates and low concentrations in the dialysate. The SmartSpecTM 3000 spectrophotometer was used to measure the concentration of dialysates sampled from the solution containing only acetate in aCSF at different flow rates. A UV-transparent cuvette with a 1 cm path length was used. The absorbance of the cuvette filled with aCSF was taken as the background. Characterization of the absorbance of acetate at different concentrations is shown in Fig. S2 in the ESI.† The absorbance at 212 nm was collected to calculate the acetate concentration in the samples.[36]

2.1.5. Fourier-transform infrared (FTIR) spectroscopy. To enable the simultaneous measurement of ethanol and its metabolites, a sample containing the three analytes was quantified using a Fourier-transform infrared (FTIR) spectrometer (Nicolet iS50, Thermo Fisher Scientific) equipped with a liquid cell (Pike Technologies) in transmission mode. The concentrations of ethanol, acetaldehyde, and acetate in the dialysate samples were measured simultaneously to calculate the recovery rates. The liquid cell's path length was set to 25 μm, which corresponds to a minimum sample volume of 30 μL. The number of scans was 180, and the spectral resolution was 0.482 cm^{-1}. The spectrum of aCSF was used as the background for absorbance calculations.

2.2. Experimental setups for *in vitro* microdialysis and backpressure measurement

Fig. 1(a) shows the experimental setup of the *in vitro* microdialysis experiment. The setup used in this research is similar to a previously published work.[34] In short, a 100 mL media bottle was used to contain different compounds prepared in aCSF to simulate the brain environment after ethanol administration and investigate the performance of the probe. The probe was dipped into the solution through a hole drilled on the cap which was sealed to minimize evaporation of the standard solution. A hotplate (Fisherbrand™ Isotemp™, Thermo Fisher Scientific) was used to heat up the solution and maintain the temperature at 37 °C which was monitored by a thermometer. A magnetic stirrer was used to ensure uniform temperature and concentration distribution throughout the solution. A syringe pump (11 Elite, Harvard Apparatus) was connected to the inlet of the probe to perfuse aCSF during microdialysis. At the outlet, a 250 μL centrifuge tube, which was placed in ice to minimize evaporation during the sample collection process, was used to collect the dialysate. Finally, the collected samples were analyzed using a UV spectrometer, FTIR spectrometer and GC-FID for quantification.

Backpressure builds up when pumping fluid into a microdialysis probe due to the long and narrow inlet and outlet tubing. Knowing how much backpressure can be withstood by the probe is critical for experimental design since high backpressure tends to cause ultrafiltration (leakage of fluid out of the membrane to the surrounding medium due to the pressure gradient across the membrane) which can lead to erroneous results and misinterpretation of data. To measure the backpressure in a probe, a uPS (LabSmith) pressure sensor was connected closely to the probe inlet on one end and to the syringe pump on the other end as shown in Fig. 1(b). In the experiments, aCSF was perfused at room temperature, which is 25 °C. The backpressure at the membrane was determined by subtracting the pressure drop between the probe inlet and the membrane from the measured pressure. This pressure drop can be calculated using the Hagen–Poiseuille equation by considering the perfusion flow rate, viscosity, and dimensions of the probe. The uProcess™ software

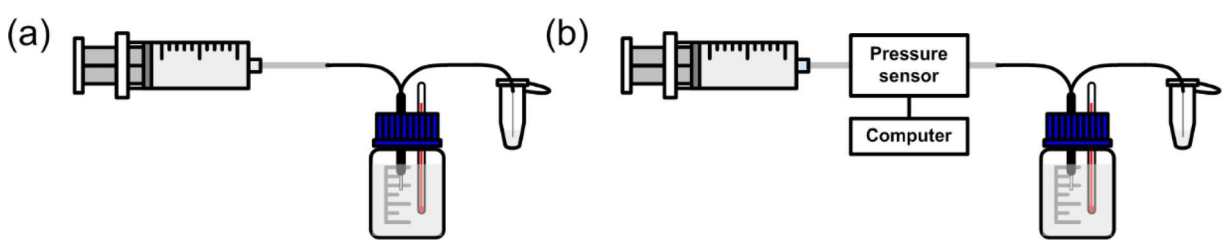

Fig. 1 (a) Experimental setup for *in vitro* microdialysis probe characterization. (b) Experimental setup for measuring backpressure of microdialysis probes.

was used in conjunction with an interface (EIB200, LabSmith) to control the device and record the data.

2.3. *In vivo* study

2.3.1. Surgery procedure for securing cannula for microdialysis probe. A female Long-Evans rat (Envigo Laboratories, Indianapolis, IN, USA), weighing 242 grams and older than 9 weeks, was anesthetized with 5% isoflurane in an induction chamber. Once it stopped moving, the rat was then transferred to a stereotaxic apparatus and the isoflurane was set to 2% through a nose cone. A guide cannula was implanted above the brain region of the striatum. A tether bolt, which was used for securing the probe during microdialysis, and the guide cannula was secured on the skull using anchor screws and dental cement. The rat was given a seven-day post-surgical recovery. All the procedures follow the NIH Guide for the Care and Use of Laboratory Animals and were approved by the Institutional Animal Care and Use Committee.

2.3.2. Ethanol self-administration training. Rats were trained to self-administer ethanol by providing 15% ethanol solutions three days a week for 24 hours for 3–5 weeks. Once intake stabilized, the rats were then switched to a 30 min limited access session to mimic the condition that would occur during microdialysis sampling.

2.3.3. *In vivo* sample collection and analysis. A lab-made probe with an active membrane length of 3 mm was inserted into the striatum of a Long-Evans rat the day before microdialysis sample collection. Before insertion, the probe was continuously perfused with aCSF at a flow rate of 1.0 μL min^{-1}. The rat was conscious and freely moving during the experiment. The flow rate was then lowered to 0.1 μL min^{-1} overnight. The flow rate was increased to 1.0 μL min^{-1} two hours before starting sample collection. A bottle containing 15% ethanol solution was provided to the rat, with sample collection intervals set at 10 minutes increments for a duration of two hours and 30 minutes. This included the collection of three baseline samples prior to ethanol administration. A gas chromatograph (GC, 430-GC, Bruker) equipped with a flame ionization detector (FID) and an autosampler (COMBI PAL-xt) was used to measure ethanol, acetaldehyde and acetate in the brain dialysate samples. A capillary column (30 m × 0.53 mm × 1 μm film thickness) was used, with helium as the carrier gas with a flow rate set at 8.5 mL min^{-1}. A carboxen/PDMS coated solid phase micro-extraction (SPME) fiber (Supelco Analytical, Bellefonte, PA) was used for extraction and desorption. Acetate quantification involved esterification to methyl acetate, according to a previous study,[37] followed by the analysis of methyl acetate using headspace gas chromatography. In this process, 1 μL of sulfuric acid and 1 μL of methanol were added to a 5 μL acetate solution in a conical gas vial, sealed with a septum, and incubated at 50 °C for 45 minutes. After cooling on ice, 2 μL of the mixture was transferred to a GC vial for quantification. The sample volume for ethanol and acetaldehyde was also 2 μL. The oven temperatures for ethanol, acetaldehyde, and methyl acetate were set at 65 °C, 30 °C, and 75 °C, respectively. The incubation temperatures were 35 °C for ethanol, 25 °C for acetaldehyde, and 35 °C for methyl acetate. The injector temperature was maintained at 220 °C. The extraction times were 3 minutes for ethanol, 5 minutes for acetaldehyde, and 3 minutes for methyl acetate, with a desorption time of 1 minute for all analytes. Calibration details of the GC-FID for *in vivo* experiments using ethanol, acetaldehyde, and methyl acetate solutions at varying concentrations are provided in the ESI, Fig. S4.†

2.4. Numerical simulations

3D models of the probe were constructed according to its geometry and configuration using a commercially available finite-element multiphysics simulation software (COMSOL 5.4) with a computational fluid dynamics (CFD) module. Both convection and diffusion effects were solved in the Laminar Flow Module coupled with the Transport of Diluted Species Module. The flow was assumed to be laminar throughout the probe due to small dimensions and slow flow velocity, resulting in a small Reynolds number (Re < 10). To simulate the recovery rate of the probes under the same experimental conditions, a constant concentration of 20 mM was applied to the surface of the membrane as a boundary condition for two reasons: the concentration in the surrounding is uniform due to well-mixing condition, and the loss of ethanol molecules can be neglected due to the large reservoir volume.

As the analytes diffuse into the probe, their concentration in the brain decreases, and if the rate of diffusion into the probe is higher than the rate of diffusion from the brain into the region in the vicinity of the probe, then a lower local concentration of the analyte is established in a volume of tissue adjacent to the probe membrane. To simulate this depletion effect in the rat brain during *in vivo* microdialysis, a simplified cylinder model with a 2 mm radius and 3 mm height was used to represent the sampled brain region which has a similar volume as the rat striatum.[38] The model configuration is shown in the ESI in Fig. S5.† A constant concentration boundary condition was applied to the boundary of the brain. The diffusion coefficient of analytes in the brain was assumed to be approximately the same as that in water due to limited information in published papers.

3. Results and discussion

3.1. Recovery rate as a function of flow rate

Characterization of microdialysis probes with different configurations can help with understanding their performance, which is important for experimental design and optimization. One important parameter that can be used to quantify the performance of the probes is the analyte recovery rate, which is defined as the analyte concentration of the sample collected at the outlet (in dialysate) *versus* the analyte concentration in the external medium.

In this study, three different probes were directly compared: a lab-made probe, a commercial MAB probe and a CMA probe. The details of the probes and their schematics are provided in Fig. 2. These probes with different membrane materials were used to measure the recovery rates of ethanol, acetate, and

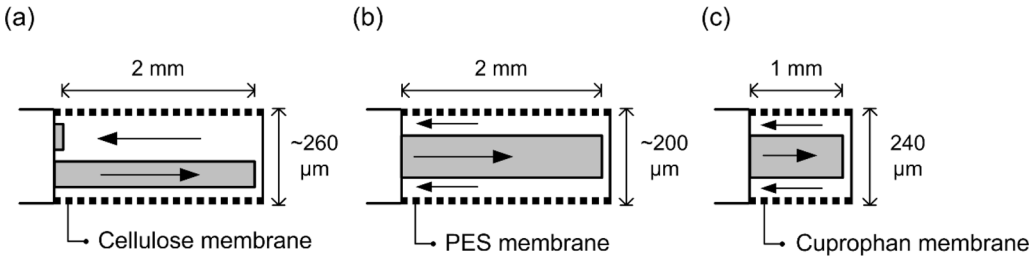

Fig. 2 Schematic of (a) a lab-made probe, (b) a commercial MAB probe and (c) a commercial CMA probe. The membrane lengths and diameter are specified for each probe.

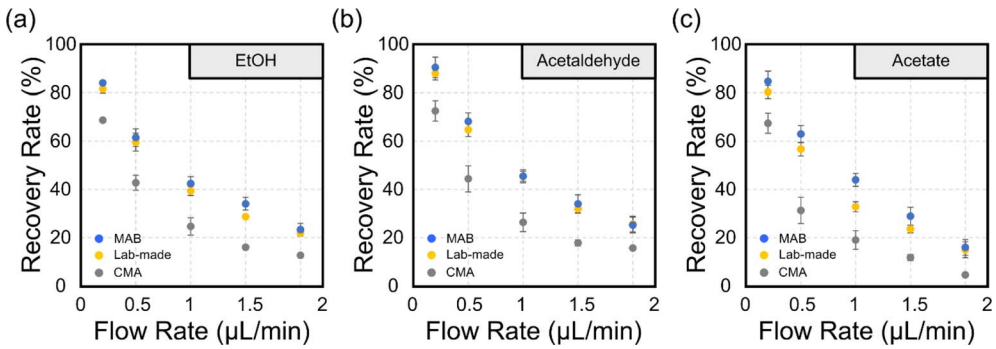

Fig. 3 Recovery rate at a constant concentration of 20 mM of the surrounding medium for (a) ethanol, this data was previously published by our group[34] (b) acetaldehyde, and (c) acetate at different flow rates. All the error bars represent the standard deviation ($N = 3$). At some datapoints, the error bars are too small to visibly see.

acetaldehyde at different flow rates, to allow for direct comparison.

Fig. 3(a)–(c) show the recovery rates of ethanol, acetaldehyde, and acetate for different flow rates, using the lab-made probe, commercial MAB probe and commercial CMA probe, respectively. In general, higher recovery rates were observed for slower flow rates as expected since slowing down the flow rate allows more time for molecules to diffuse into the membrane. For flow rates above 1 μL min^{-1} the recovery rates are very low, below 20%.

Acetaldehyde showed the highest recovery rates for all probes, followed by ethanol and then acetate. This agrees with previous work by Chen *et al.*[39] who showed that smaller molecules have higher diffusion coefficients in the membrane, resulting in a higher recovery rate. Additionally, probes with different membrane materials and configurations show different performance. Since the pore sizes of the three membranes are much bigger than the size of the molecules, the effect of pore size on the performance is not significant, which is verified in the later section of numerical simulation. Since no clear difference in terms of recovery rate is observed between different configurations of the probes, the results may suggest a minor effect of probe configuration design on its performance. CMA probes have the lowest recovery rates compared to the other two probes due to the shorter membrane length. These results provide information on the performance of the probes for individual analytes, thus offering deeper insight into the data interpretation of the simultaneous measurement of the three analytes in the following section.

3.2. Recovery rates for simultaneous microdialysis sampling of ethanol, acetaldehyde and acetate

The ability to simultaneously sample ethanol, acetaldehyde, and acetate is crucial in advancing our understanding of the effects of ethanol metabolites, which has not been demonstrated using microdialysis to date. In this *in vitro* test, simultaneous sampling of the mixture of ethanol, acetaldehyde, and acetate, each at a concentration of 20 mM was performed using the lab-made microdialysis probe.

The analysis to determine the concentrations of each compound in the dialysate were performed using a Fourier transform infrared spectrometer (FTIR) with a liquid cell having a path length of 25 μm. Absorbance spectra of mixtures containing 5, 10, 15, and 20 mM for each analyte were used to relate an absorbance peak of each compound to its concentration, as shown in the ESI in Fig. S4.† The symmetric C–O stretching peak around 1046 cm^{-1}, C–O stretching peak around 1175 cm^{-1}, and C–O stretching peak around 1280 cm^{-1} were used for the quantification of ethanol, acetaldehyde, and acetate, respectively. A flow rate of 1 μL min^{-1} was selected as it reduces the sample collection time and minimizes evaporation of the analytes in the dialysates while being collected, while maintaining a high enough recovery rate to detect individual analytes using infrared spectroscopy.

The recovery rates of ethanol, acetaldehyde, and acetate are shown in Table 1. The results obtained from three different probes with three repeats are presented as an average followed by standard deviation. The recovery rates of each analyte in the

Table 1 Recovery rates for each compound within a mixture containing 20 mM of ethanol, 20 mM of acetaldehyde, and 20 mM of acetate

	Probe 1	Probe 2	Probe 3
Ethanol	38.7 ± 2.2%	37.2 ± 1.1%	36.4 ± 1.4%
Acetaldehyde	43.2 ± 2.1%	38.6 ± 1.7%	41.5 ± 2.7%
Acetate	38.1 ± 1.6%	35.6 ± 1.4%	33.9 ± 2.3%

mixture are comparable (within 10% difference) to those measured individually, which may indicate that there is no significant interaction between the analytes. Furthermore, the successful demonstration of applying microdialysis to a mixture suggests the possibility of sampling multiple analytes simultaneously without compromising accuracy.

While the concentration of ethanol used in this study falls within the physiological range, the concentrations of the other two metabolites, acetaldehyde and acetate, are higher than the physiological levels. This fact should not affect the microdialysis recovery rates of ethanol, acetaldehyde, and acetate. Considering the capability of infrared spectroscopy to measure the three compounds, more work needs to be done in order to optimize the measurement configuration of the infrared technique and to determine the limits of detection before it can be used for analysis of *in vivo* dialysate samples.

3.3. *In vivo* microdialysis in rat brain

In order to demonstrate the changes of ethanol, and its metabolites acetaldehyde and acetate, in the brain, *in vivo* microdialysis was performed during and after alcohol consumption. In Fig. 4, a 15% ethanol solution was provided at time zero. During the 30 minute drinking session, 0.32 g kg^{-1} of ethanol was consumed by the rat. Fig. 4 shows the time course concentration of ethanol, acetaldehyde and acetate in the rat brain dialysate. In the figure, the concentration at "negative times" represents baseline values, and each sample concentration is presented at the midpoint of its respective collection time interval. The concentration of ethanol in the dialysate reached a maximum of 9.31 mM around 20 minutes after ethanol consumption and experienced a nearly linear decline over time. The concentration of acetaldehyde in the dialysate was approximately 100 times lower than that of ethanol. The first three acetaldehyde data points were within the noise level and thus were not included. The acetate concentration in the dialysate spiked from a baseline concentration of 0.06 mM to 0.24 mM.

The actual concentration of these compounds in the brain can be estimated using *in vitro* recovery rates values, however these may not fully account for the differences between the simulated environment and the actual brain conditions. The estimated peak concentrations of ethanol, acetaldehyde and acetate in the brain reached 16.34, 0.19 and 0.56 mM during the experiment. The time-course concentration of ethanol and its metabolites provides insights into understanding the dynamic changes in these chemicals.

3.4. Backpressure measurement

Narrow tubing with an inner diameter of tens of microns is often used to fabricate microdialysis probes. In addition, the diffusion process at the tip of the probe benefits from the small inner diameter due to the high surface-to-volume ratio. However, high pressure can easily build up when perfusing the aCSF through the probe because of the narrow inner diameter of the inlet and outlet tubing that are part of the probe. If high backpressure is present, more fluid will tend to permeate across the membrane and out of the probe. Also, high backpressure can result in failure of the syringe due to leakage of fluid behind the syringe plunger tip. The loss of fluid can lead to underestimation of recovery rate and erroneous results.

To quantify the loss of sample during microdialysis, the flow recovery rate is defined as the sample volume collected at the outlet divided by the total volume perfused by the syringe pump over a given period. As the backpressure increases, the flow

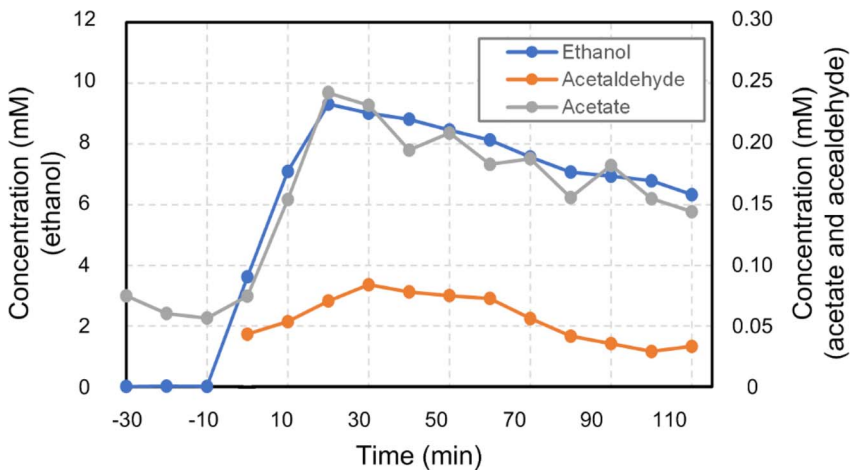

Fig. 4 Time course of dialysate concentrations of ethanol, acetaldehyde, and acetate in a rat's brain over a 2 hour period during and after alcohol consumption.

recovery rate decreases mainly due to ultrafiltration. Practically, a probe is considered unreliable if the flow recovery rate drops below 90% at any point during microdialysis.[4] Different perfusion flow rates were applied to the probes to build up different values of backpressure. Each pressure level was held for 15 minutes to ensure that the system had reached a steady state. Fig. 5(a) shows the flow recovery rate at different backpressures for both lab-made and MAB probes with 2 mm membrane length. The average maximum pressure that the lab-made and MAB probes can withstand was found to be 459.3 kPa and 145.1 kPa with a standard deviation of 40.2 kPa and 72.3 kPa, respectively. The lab-made probes showed significantly higher endurance toward the applied backpressure and more consistent performance compared to the MAB probe. Factors that may contribute to this difference between probes include ultrafiltration across the PES membrane compared with regenerated cellulose or better sealing between the membrane and tubing.

Fig. 5(b) shows the flow recovery rate at different backpressures for lab-made and CMA probes with 1 mm membrane length. The average maximum pressure that the lab-made and CMA probes can withstand was found to be 585.2 kPa and 497.7 kPa with a standard deviation of 6.8 kPa and 18.3 kPa, respectively. The difference in performance may be due to different membrane materials and fabrication processes. Higher backpressure resistance and better consistent performance were observed on probes with shorter membrane length. Probes with longer membrane lengths tend to be more affected by ultrafiltration due to the larger surface area, which is reflected in the lower flow recovery rate at a similar pressure level. As a result, both membrane length and the length of lines connecting the probe and the pump need to be optimized when designing the system to avoid incorrect interpretation of the sample due to backpressure induced ultrafiltration. Backpressure measurements were also conducted at five different flow rates, at both 25 °C and 37 °C. The variation in backpressure due to temperature was less than 5% for all measurements, as shown in Fig. S6.† Further details are provided in the ESI.†

3.5. Numerical simulations

3.5.1. Determination of diffusion coefficient of analytes in membranes. Microdialysis is a diffusion-based sampling technique. However, the diffusion coefficient in the membranes is not known and is not provided by the manufacturer, which makes it difficult to design or choose the most suitable probe for a specific application. In addition, the diffusion coefficient is an important factor for the interpretation of results and probe design. A mathematical framework for calculating concentration distribution inside and outside a concentric microdialysis probe was described in a previous study.[1] The concentration distribution can be used to determine the diffusion coefficient of analytes in different membranes. However, for side-by-side microdialysis probe geometry, the boundary conditions are more complex, and therefore mathematical calculation does not exist. For these side-by-side probes, the diffusion coefficient of analytes in different membranes can be determined numerically through regression analysis with the simulated and experimental results.[34] This method can be used for probes with either concentric or side-by-side configuration. The diffusion coefficient of each analyte is corrected to 37 °C using the Stokes-Einstein law for diffusion in solution according to another previous study to match the experimental condition.[40]

Table 2 shows both the diffusion coefficients of ethanol,[41] acetaldehyde[42] and acetate[40] in water and our results of the diffusion coefficients in membranes made of cellulose, polyethersulfone (PES), and cuprophan (CUP). The coefficient of determination for all the simulated values is greater than 0.985 indicating accurate fitting of the experimental data. The simulation shows that acetaldehyde has the highest diffusion coefficient, followed by ethanol, and acetate has the lowest diffusion coefficient in all three membranes. To compare the diffusion effect in different membrane materials, ethanol, acetaldehyde and acetate have a 12.5%, 5.1%, and 32.3% higher diffusion coefficient in PES membrane than in the cellulose membrane, respectively. The higher diffusion coefficient in the membrane results in a 7.7%, 0.1% and 34.0% higher recovery rate for ethanol, acetaldehyde and acetate respectively. The results

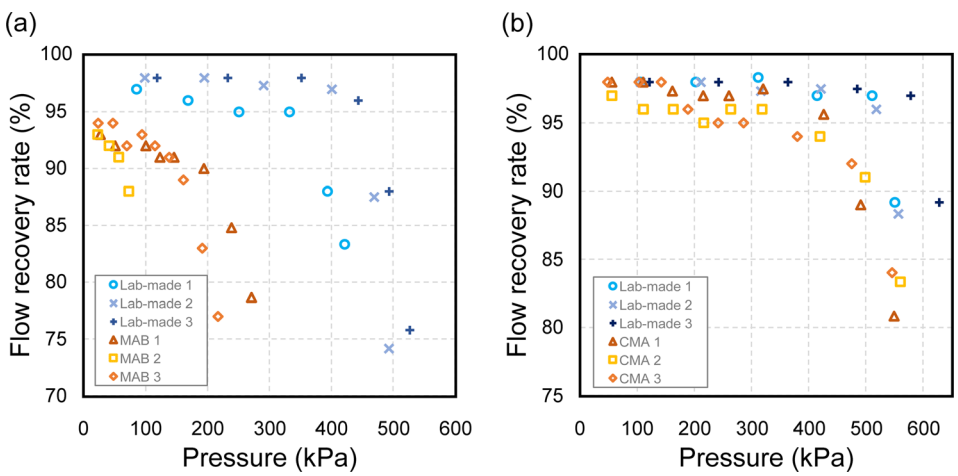

Fig. 5 Comparison of the flow recovery rate at different backpressures between lab-made and commercial probes with (a) 2 mm and (b) 1 mm membrane lengths.

Table 2 Diffusion coefficients of ethanol, acetate, and acetaldehyde in water (from literature) and in different membranes at 37 °C (determined in this study)

Diffusion coefficient	Ethanol ($\times 10^{-10}$)	Acetaldehyde ($\times 10^{-10}$)	Acetate ($\times 10^{-10}$)
In water ($m^2\ s^{-1}$)	15.8 (ref. 41)	16.3 (ref. 42)	14.8 (ref. 40)
In cellulose membrane ($m^2\ s^{-1}$)	1.2 ± 0.1	1.5 ± 0.2	1.0 ± 0.0
In PES membrane ($m^2\ s^{-1}$)	1.3 ± 0.1	1.6 ± 0.1	1.3 ± 0.1
In CUP membrane ($m^2\ s^{-1}$)	1.3 ± 0.1	1.5 ± 0.2	1.1 ± 0.1

imply a close correlation between the diffusion coefficient of analytes in the membrane and the recovery rate.

3.5.2. Depletion region of different analytes. The microdialysis process constantly depletes the molecules adjacent to the membrane surface, which results in a varying concentration distribution of the analytes in the nearby region, *i.e.*, in the tissue. However, it is challenging to study this depletion effect experimentally. In this work, through numerical modeling, we have quantified the extent of the depletion in the tissue as a function of time for the three analytes. The depletion region was used to quantify the depletion effect, and it was defined as the radial distance from the probe where the concentration of the analyte in the tissue drops to 90% of the concentration compared to the concentration where there is no perfusion flow in the probe.

Fig. 6(a)–(c) show the simulated depletion region for ethanol, acetaldehyde, and acetate, respectively, as a function of sampling time and flow rate. These results are for the lab-made probe model with a 2 mm membrane length. After an hour of sampling, the depletion region reaches a steady state (where variation is less than 1% over 5 minutes) and the extent of the depletion region reaches around 600 μm away from the probe. Steady state is reached when the number of molecules leaving the tissue to the microdialysis probe is equal to the number of

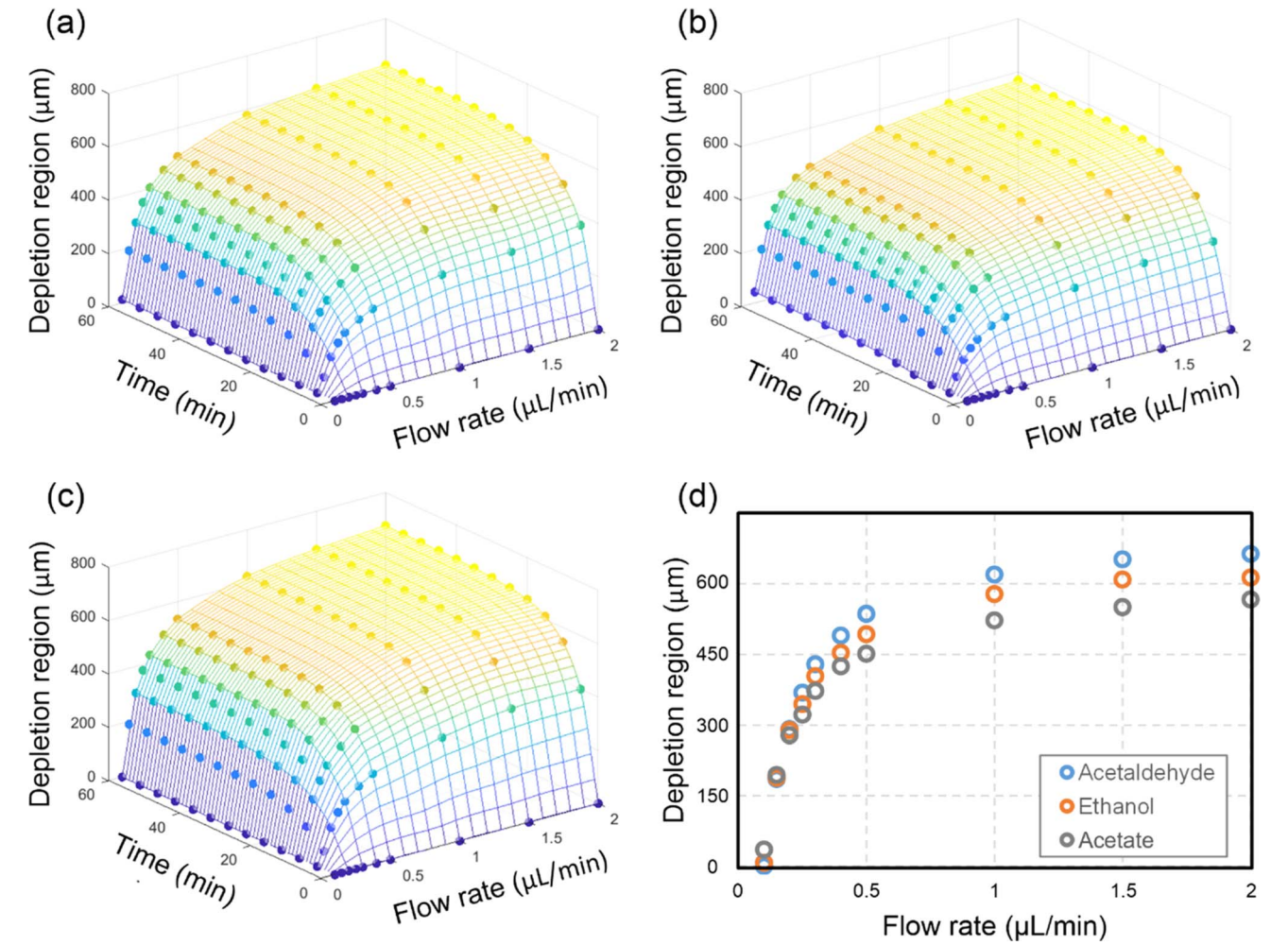

Fig. 6 Simulated depletion region for different times and different flow rates for (a) ethanol, (b) acetate and (c) acetaldehyde. (d) Depletion region for different flow rates after 30 minutes of continuous microdialysis sampling.

molecules arriving to the region near the probe from the surrounding tissue, which depends on the diffusion coefficient of the analyte in the tissue.

The depletion time is defined as the time needed for the depletion region to evolve from the beginning to 90% of its steady-state extent. The depletion time for all three analytes decreases significantly when the flow rate increases. For ethanol, the depletion time drops from 43.7 to 16.2 minutes when the flow rate increases from 0.1 to 2 μL min^{-1}. A higher flow rate removes molecules that diffuse into the membrane, and this leads to a higher concentration gradient across the membrane, and this results in more significant depletion.

Fig. 6(d) shows the dependence of flow rate on depletion for ethanol, acetaldehyde, and acetate. For flow rates higher than 0.2 μL min^{-1}, acetaldehyde has the largest depletion region while acetate has the smallest. However, for flow rates lower than 0.2 μL min^{-1}, the results are reversed. According to Fick's first law, the concentration gradient is proportional to mass flux over diffusion coefficient, which is equivalent to recovery rate over diffusion coefficient at a constant flow rate. The recovery rate ratio between two analytes at different flow rates is not constant. At high flow rate, the ratio is smaller than that at low flow rate. As a result, the concentration gradient ratio between two analytes varies at different flow rates, causing the relative size of the depletion region to vary at different flow rates.

The effect of concentration on the depletion region is not significant for ethanol and its metabolites. In the case of performing 30 minutes of sampling, the depletion region drops by less than 4% as the concentration in the surrounding decreases from 20 to 0.1 mM. For probes with different configurations, the depletion effect was studied using ethanol at 20 mM as an analyte. After sampling for 30 minutes at 2 μL min^{-1}, no significant difference in terms of depletion region was observed. The lab-made probe with a side-by-side configuration has a depletion region of 613 μm, and the MAB probe with a concentric configuration has a depletion region of 627 μm, which is within a 3% difference.

4. Conclusions

The performance of microdialysis probes, in terms of recovery rate, with different configurations and membrane materials, was characterized *in vitro* for ethanol, acetaldehyde and acetate at different flow rates. Simultaneous measurement of all the analytes at 20 mM was achieved using infrared spectroscopy, where the collected spectra were directly used for analysis without pre-processing. The estimated recovery rate for each analyte, when they were in the same external solution, was comparable to that measured for each analyte individually, confirming the possibility of accurately sampling multiple analytes simultaneously. *In vivo* microdialysis was performed, and the time course response after ethanol consumption was monitored, demonstrating the measurement of ethanol, acetaldehyde and acetate.

The experimental data, combined with numerical simulations, were used to determine the diffusion coefficients of ethanol and its metabolites in different membranes. Acetaldehyde had the highest diffusion coefficient, followed by ethanol and then acetate. The combination of experimental data and numerical simulation could also be used to determine diffusion coefficients for other small molecules.

The evolution of a depletion zone around the microdialysis probe was studied numerically as a function of time for different flow rates, different analytes and probes. The perfusion flow rate and sampling time were the determining factors for the evolution of the depletion region, while the configuration of the probe and the concentration in the surrounding had only a minor effect. Additionally, the flow recovery rate of the probe was measured at different backpressures to quantify the maximum pressure the probe could withstand, which is important when setting up the microdialysis experiment system.

Data availability

The data supporting this article have been included as part of the ESI.†

Conflicts of interest

The authors declare no conflict of interest.

Acknowledgements

Research reported in this publication was supported by the National Institute on Alcohol Abuse and Alcoholism (NIAAA) of the National Institutes of Health (NIH) under Award Number R21AA029770. The content is solely the responsibility of the authors and does not necessarily represent the official views of the National Institutes of Health. The authors would like to acknowledge Joanne Lee for training the rats to self-administer ethanol, and Regina Mangieri for providing access to a gas chromatography instrument. Tse-Ang Lee would like to acknowledge the financial support provided by the Fred Murphy Jones and Homer Lindsey Bruce Endowed Fellowship from the Waggoner Center for Alcohol and Addiction Research at The University of Texas at Austin.

References

1 P. M. Bungay, P. F. Morrison and R. L. Dedrick, Steady-state theory for quantitative microdialysis of solutes and water in vivo and in vitro, *Life Sci.*, 1990, **46**(2), 105–119.
2 H. O. Pettit and J. B. Justice, Chapter 6 - Procedures for microdialysis with smallbore HPLC, in *Techniques in the Behavioral and Neural Sciences*, ed. T. E. Robinson and J. B. Justice, Elsevier, 1991, vol. 7, pp. 117–53.
3 F. C. Alimagham, D. Hutter, N. Marco-García, E. Gould, V. H. Highland, A. Huefner, *et al.*, Cerebral Microdialysate Metabolite Monitoring using Mid-infrared Spectroscopy, *Anal. Chem.*, 2021, **93**(35), 11929–11936.
4 C. J. Schier, R. A. Mangieri, G. A. Dilly and R. A. Gonzales, Microdialysis of Ethanol During Operant Ethanol Self-

administration and Ethanol Determination by Gas Chromatography, *J. Visualized Exp.*, 2012, (67), 4142.
5 S. Kim, E. Y. Jang, S. H. Song, J. S. Kim, I. S. Ryu, C. H. Jeong, *et al.*, Brain Microdialysis Coupled to LC-MS/MS Revealed That CVT-10216, a Selective Inhibitor of Aldehyde Dehydrogenase 2, Alters the Neurochemical and Behavioral Effects of Methamphetamine, *ACS Chem. Neurosci.*, 2021, **12**(9), 1552–1562.
6 P. Tůma, Steady state microdialysis of microliter volumes of body fluids for monitoring of amino acids by capillary electrophoresis with contactless conductivity detection, *Anal. Chim. Acta*, 2024, **1287**, 342113.
7 Y. Chen, D. i. Graham and T. w Stone, Release of endogenous adenosine and its metabolites by the activation of NMDA receptors in the rat hippocampus in vivo, *Br. J. Pharmacol.*, 1992, **106**(3), 632–638.
8 S. Dietze and K. Kuschinsky, Determination of extracellular glutamate after local K+ stimulation in the striatum of non-anaesthetised rats after treatment with dopaminergic drugs—studies using microdialysis, *J. Neural Transm. Gen. Sect.*, 1992, **90**(1), 1–11.
9 H. Hagberg, P. Andersson, J. Lacarewicz, I. Jacobson, S. Butcher and M. Sandberg, Extracellular Adenosine, Inosine, Hypoxanthine, and Xanthine in Relation to Tissue Nucleotides and Purines in Rat Striatum During Transient Ischemia, *J. Neurochem.*, 1987, **49**(1), 227–231.
10 C. Okuda, T. Sawa, M. Harada, T. Murakami, T. Matsuda and Y. Tanaka, Lactate in rat skeletal muscle after hemorrhage measured by microdialysis probe calibrated in situ, *Am. J. Physiol.: Endocrinol. Metab.*, 2006, **263**(6), E1035–E1039.
11 R. Kuczenski and D. Segal, Concomitant characterization of behavioral and striatal neurotransmitter response to amphetamine using in vivo microdialysis, *J. Neurosci.*, 1989, **9**(6), 2051–2065.
12 M. T. Bowser and R. T. Kennedy, In vivo monitoring of amine neurotransmitters using microdialysis with on-line capillary electrophoresis, *Electrophoresis*, 2001, **22**(17), 3668–3676.
13 E. Toth, H. Sershen, A. Hashim, E. S. Vizi and A. Lajtha, Effect of nicotine on extracellular levels of neurotransmitters assessed by microdialysis in various brain regions: Role of glutamic acid, *Neurochem. Res.*, 1992, **17**(3), 265–271.
14 P. J. Hutchinson, I. Jalloh, A. Helmy, K. L. H. Carpenter, E. Rostami, B. M. Bellander, *et al.*, Consensus statement from the 2014 International Microdialysis Forum, *Intensive Care Med.*, 2015, **41**, 1517–1528.
15 M. G. Stovell, A. Helmy, E. P. Thelin, I. Jalloh, P. J. Hutchinson and K. L. H. Carpenter, An overview of clinical cerebral microdialysis in acute brain injury, *Front. Neurol.*, 2023, **14**, 1085540.
16 H. K. Seitz and F. Stickel, Acetaldehyde as an underestimated risk factor for cancer development: role of genetics in ethanol metabolism, *Genes Nutr.*, 2010, **5**(2), 121–128.
17 D. W. Crabb, W. F. Bosron and T. K. Li, Ethanol metabolism, *Pharmacol. Ther.*, 1987, **34**(1), 59–73.
18 F. E. Ahmed, Toxicological Effects of Ethanol on Human Health, *Crit. Rev. Toxicol.*, 1995, **25**(4), 347–367.
19 Z. A. Rodd-Henricks, R. I. Melendez, A. Zaffaroni, A. Goldstein, W. J. McBride and T. K. Li, The reinforcing effects of acetaldehyde in the posterior ventral tegmental area of alcohol-preferring rats, *Pharmacol., Biochem. Behav.*, 2002, **72**(1–2), 55–64.
20 A. Vonlaufen, J. S. Wilson, R. C. Pirola and M. V. Apte, Role of Alcohol Metabolism in Chronic Pancreatitis, *Alcohol Res. Health*, 2007, **30**(1), 48–54.
21 Y. E. Cho, E. Mezey, J. P. Hardwick, Jr. N. Salem, D. L. Clemens and B. J. Song, Increased ethanol-inducible cytochrome P450-2E1 and cytochrome P450 isoforms in exosomes of alcohol-exposed rodents and patients with alcoholism through oxidative and endoplasmic reticulum stress, *Hepatol. Commun.*, 2017, **1**(7), 675–690.
22 M. Pardo, A. Betz, N. San Miguel, L. López-Cruz, J. Salamone and M. Correa, Acetate as an active metabolite of ethanol: studies of locomotion, loss of righting reflex, and anxiety in rodents, *Front. Behav. Neurosci.*, 2013, **7**, 81.
23 P. Mews, G. Egervari, R. Nativio, S. Sidoli, G. Donahue, S. I. Lombroso, *et al.*, Alcohol metabolism contributes to brain histone acetylation, *Nature*, 2019, **574**(7780), 717–721.
24 M. Nurmi, K. Kiianmaa and J. D. Sinclair, Brain ethanol in AA, ANA, and Wistar rats monitored with one-minute microdialysis, *Alcohol*, 1994, **11**(4), 315–321.
25 G. Theodoridis, E. H. M. Koster and G. J. de Jong, Solid-phase microextraction for the analysis of biological samples, *J. Chromatogr. B: Biomed. Sci. Appl.*, 2000, **745**(1), 49–82.
26 M. P. Lam, P. W. Marinelli, L. Bai and C. Gianoulakis, Effects of acute ethanol on opioid peptide release in the central amygdala: an in vivo microdialysis study, *Psychopharmacology*, 2008, **201**(2), 261–271.
27 R. Sharma, S. C. Engemann, P. Sahota and M. M. Thakkar, Effects of Ethanol on Extracellular Levels of Adenosine in the Basal Forebrain: An In Vivo Microdialysis Study in Freely Behaving Rats, *Alcohol: Clin. Exp. Res.*, 2010, **34**(5), 813–818.
28 R. I. Melendez, Z. A. Rodd-Henricks, E. A. Engleman, T. K. Li, W. J. McBride and J. M. Murphy, Microdialysis of Dopamine in the Nucleus Accumbens of Alcohol-Preferring (P) Rats During Anticipation and Operant Self-Administration of Ethanol, *Alcohol: Clin. Exp. Res.*, 2002, **26**(3), 318–325.
29 M. Jamal, K. Ameno, M. Kumihashi, S. Ameno, T. Kubota, W. Wang, *et al.*, Microdialysis for the determination of acetaldehyde and ethanol concentrations in the striatum of freely moving rats, *J. Chromatogr. B*, 2003, **798**(1), 155–158.
30 O. Sørensen, A. Andersen, H. Olsen, K. Alexandr, P. O. Ekstrøm, K. E. Giercksky, *et al.*, Validation and use of microdialysis for determination of pharmacokinetic properties of the chemotherapeutic agent mitomycin C - an experimental study, *BMC Cancer*, 2010, **10**(1), 469.
31 M. Kveim and J. E. Bredesen, A gas chromatographic method for determination of acetate levels in body fluids, *Clin. Chim. Acta*, 1979, **92**(1), 27–32.
32 M. F. Laker and M. A. Mansell, Measurement of Acetate in Aqueous Solutions and Plasma by Gas Phase

Chromatography using a Porous Polymer Stationary Phase, *Ann. Clin. Biochem. Int. J. Lab. Med.*, 1978, **15**(1–6), 228–232.

33 T. A. Lee, J. Peng, G. Kowal, R. Gonzales and T. Hutter, Infrared spectroscopy for neurochemical monitoring of alcohol and its metabolites, in *Frontiers in Biological Detection: From Nanosensors to Systems XV*, SPIE, 2023, vol. 12397, pp. 20–24.

34 T. A. Lee, R. Gonzales and T. Hutter, Parametric study of a microdialysis probe and study of depletion effect using ethanol as a test analyte, *Biochem. Biophys. Res. Commun.*, 2022, **637**, 136–143.

35 S. L. Zandy, J. M. Doherty, N. D. Wibisono and R. A. Gonzales, High sensitivity HPLC method for analysis of in vivo extracellular GABA using optimized fluorescence parameters for o-phthalaldehyde (OPA)/sulfite derivatives, *J. Chromatogr. B: Anal. Technol. Biomed. Life Sci.*, 2017, **1055–1056**, 1–7.

36 G. Ruderman, E. R. Caffarena, I. G. Mogilner and E. J. Tolosa, Hydrogen Bonding of Carboxylic Acids in Aqueous Solutions—UV Spectroscopy, Viscosity, and Molecular Simulation of Acetic Acid, *J. Solution Chem.*, 1998, **27**, 935–948.

37 H. G. Giles, S. Meggiorini and E. I. Vidins, Semiautomated analysis of ethanol and acetate in human plasma by head space gas chromatography, *Can. J. Physiol. Pharmacol.*, 1986, **64**(6), 717–719.

38 J. W. Hsu, L. C. Lee, R. F. Chen, C. T. Yen, Y. S. Chen and M. L. Tsai, Striatal volume changes in a rat model of childhood attention-deficit/hyperactivity disorder, *Psychiatry Res.*, 2010, **179**(3), 338–341.

39 K. C. Chen, M. Höistad, J. Kehr, K. Fuxe and C. Nicholson, Theory relating in vitro and in vivo microdialysis with one or two probes: General theory for microdialysis, *J. Neurochem.*, 2002, **81**(1), 108–121.

40 G. Rudelstorfer, M. Siebenhofer and A. Grafschafter, Modeling of Single Droplet Mass Transfer of Acetic Acid with Triisooctylamine-Based Solvent, *Chem. Ing. Tech.*, 2021, **93**(10), 1509–1517.

41 E. E. Hills, M. H. Abraham, A. Hersey and C. D. Bevan, Diffusion coefficients in ethanol and in water at 298K: Linear free energy relationships, *Fluid Phase Equilib.*, 2011, **303**(1), 45–55.

42 M. L. Mansfield, Mass Transport of Gases across the Air–Water Interface: Implications for Aldehyde Emissions in the Uinta Basin, Utah, USA, *Atmosphere*, 2020, **11**(10), 1057.

